

Article

The Influence of pH on Subsurface Denitrification Stimulated with Emulsified Vegetable Oil

Veronica L. Gonzalez ¹, Paul M. Dombrowski ^{1,2}, Michael D. Lee ³ and C. Andrew Ramsburg ^{1,*} ¹ Department of Civil & Environmental Engineering, Tufts University, Medford, MA 02155, USA² In-Situ Oxidative Technologies, Inc. (ISOTEC), Lawrenceville, NJ 08648, USA³ Terra Systems, Inc., Wilmington, DE 19809, USA

* Correspondence: andrew.ramsburg@tufts.edu; Tel.: +1-617-627-4286

Abstract: Treatment of nitrate rich groundwater using permeable reactive barriers (PRBs) established with injection of emulsified vegetable oil is receiving attention in areas where groundwater discharges contribute to eutrophication (e.g., Cape Cod, MA). To better understand the biogeochemical process kinetics when emulsified vegetable oil (EVO) is used to stimulate denitrification within the subsurface, microcosm experiments and process-based modeling were conducted for pH conditions ranging from 4 to 8. Biomass variability in soil and pH variations were found to affect denitrification, with limited nitrate reduction observed below pH 5.0. Different rates for denitrification associated with biomass variability suggest that a greater characterization of the indigenous biological community may improve PRB design and operation. Process-based modeling employed the activated sludge model No 3 (AMS3) framework that assumes denitrification as a two-step anoxic process dependent primarily on heterotrophic bacteria, soluble substrate, nitrate, and nitrite. Experimental data were used to calibrate the model under neutral to low pH, resulting in a robust set of equations that can be coupled with transport in future research to improve PRB effectiveness.

Keywords: denitrification; nitrate; emulsion; permeable reactive barrier; biostimulation; EVO; ASM; process-based denitrification model

**Citation:** Gonzalez, V.L.;

Dombrowski, P.M.; Lee, M.D.;

Ramsburg, C.A. The Influence of pH on Subsurface Denitrification Stimulated with Emulsified Vegetable Oil. *Water* **2023**, *15*, 883. <https://doi.org/10.3390/w15050883>

Academic Editor: Shengrui Wang

Received: 25 January 2023

Revised: 11 February 2023

Accepted: 21 February 2023

Published: 24 February 2023



Copyright: © 2023 by the authors. Licensee MDPI, Basel, Switzerland. This article is an open access article distributed under the terms and conditions of the Creative Commons Attribution (CC BY) license (<https://creativecommons.org/licenses/by/4.0/>).

1. Introduction

Nitrogen is the most common groundwater contaminant worldwide [1], frequently present as nitrate (NO_3^-) and nitrite (NO_2^-). The main sink of nitrogen in water is denitrification—the process where bacteria use NO_3^- as a terminal electron acceptor in their metabolic processes [2]. Denitrification can occur naturally in any environment but is enhanced through engineering measures that often involve the addition of short chain, organic carbon compounds (use of methanol and glycerol products is common at water resource recovery facilities) [3].

Technologies to leverage denitrification in groundwater include injection of organic substrate in a grid of wells to reduce or retain plumes [4,5], soil aquifer treatment [6], natural attenuation in nearshore marine sediments [7], and permeable reactive barriers (PRBs) [1]. PRBs are most often designed to treat hazardous contaminants in groundwater under natural gradient conditions [8]. Constructed transverse to the flow, PRBs are traditionally installed as a continuous trench, though direct injection of reactive material can be used when the reactive material and water table allow injection approaches (e.g., limestone, zero valent iron, activated carbon and emulsified oils) [9]. PRBs have traditionally been used to treat (reduce) halogenated hydrocarbons, hexavalent chromium, arsenic, and uranium. However, early field trials performed by Robertson and Cherry [10] using trenches filled with sawdust suggested a significant attenuation (60–100%) of nitrate levels and potential for long-term treatment without replacement of the reactive material. For biological treatment of nitrate, the organic carbon necessary to enhance denitrification is supplied as the reactive medium. For PRBs established with emulsified vegetable oil (EVO), the reactive

zone comprises locations where dispersed phase emulsion is retained within the porous medium. Emulsified vegetable oils hold promise for stimulating denitrification based on their use in stimulating microbial communities within the context of bioremediation of chlorinated organic compounds and metals [11–14]. With respect to using emulsions to create a PRB, Lee et al. [15] found that larger droplet sizes favored emulsion retention to sustain nitrate reduction longer, which is consistent with results from studies demonstrating emulsion transport in sandy porous medium [16–18]. Moreover, treatment zones can be created using oil-in-water emulsions that are designed for retention at levels that limit flow bypass [19–21].

Since the 1930s, Cape Cod (Massachusetts, USA) has faced the challenge of reducing the impact of nitrogen in water due to the widespread use of septic disposal systems [22,23]. These septic systems have created numerous nitrate plumes in a hydrogeologic setting that supports relatively rapid transport and limited attenuation before groundwater discharges to coastal waters or lakes. A study from Rakhimbekova et al. [24] outlines the challenges in predicting this attenuation near groundwater–lake interfaces due to high spatiotemporal variability in the geochemical conditions.

More than one third of Cape Cod's gross regional product comes from tourism-related industries and other activities that are directly affected by eutrophication and nitrogen contamination [23]. Therefore, a regional plan was created to address federal regulatory requirements under the Clean Water Act and to develop combined strategies aimed at reducing eutrophication, fish kills, and diminished shellfisheries by decreasing the flux of nitrate entering surface water bodies. The Cape Cod Area Wide Water Quality Management Plan [23] includes PRBs as an alternative technology for the region to reduce and control nitrogen using innovative technology. The plan explores opportunities to avoid large investments in constructing wastewater treatment systems that would represent a large pressure on the public and individual finances within communities on Cape Cod. One concern for PRB implementation on Cape Cod is groundwater pH that ranges from 4.0 and 5.0 at some potential PRB sites. The pH range preferred by heterotrophic denitrifiers is generally thought to be between 5.5 and 8.0, and denitrification rates can decrease significantly in pH levels below 4.6 and above 8.3 [25].

While there has been considerable research on the use of emulsified oil as a fermentable substrate to support growth of populations of dechlorinating bacteria [12,26–29], studies focusing on using emulsified oil for denitrification are limited. While we are not aware of any study that examined the process kinetics associated with supporting denitrification through addition of emulsified oil, the use of emulsified oil as electron donor has been characterized. Among the more sophisticated approaches is that of Gihring et al. [30] and Tang et al. [13]. These studies examined the use of EVO for biostimulation during treatment of uranium contaminated groundwater. Their conceptual model describing oil hydrolysis was a complex, multistep process that resulted in slow and sustained production of acetate and hydrogen.

Denitrification in porous media has been examined in batch experiments [31–33], column experiments [34–39] and field studies [40,41]. The most common approach to model bioactivity is the use of Monod type expressions. Yet, these approaches typically do not include the level of process or stoichiometric sophistication found in the process-based models available in the wastewater treatment literature.

The overall objective of this work is to elucidate biokinetics of denitrification within microcosms stimulated with emulsified vegetable oil. Of particular interest is the influence pH may have on the biostimulation process that must occur when engineering denitrification treatment via the PRB approach. Additionally, this work aims to mathematically describe, using activated sludge model No 3 (ASM3) framework, the denitrification occurring in the microcosm experiments. The ASM3 framework offers valuable perspective on bioprocesses related to nitrification and denitrification [42–45]. While the ASM3 model framework employs a two-step denitrification model, recent studies have illustrated how molecular tools can identify and further refine the role of denitrifiers particularly related to intermediate,

reduced nitrogen species link bioprocesses with bacteria [3,46,47]. The research described herein aims to contribute process-rate information related to the engineered reduction of nitrate within the subsurface. While this study employs sediments collected from Cape Cod, the focus on process rates enables broader application. The rates of carbon utilization and nitrate reduction may be coupled with information on microbial communities and the distribution of the emulsified oil to support the design of denitrifying PRBs.

2. Materials and Methods

2.1. Materials

Potassium nitrate, potassium nitrite, ammonium chloride, hydrochloric acid, and sodium hydroxide were purchased from Fisher Scientific (Waltham, MA, USA). Chemical oxygen demand (COD) standard solution was purchased from HACH (Loveland, CO, USA). Purified water (resistivity ≥ 18.2 m Ω ·cm and total organic carbon (TOC) ≤ 8 ppb) was obtained from a Milli-Q Gradient A-10 station (Millipore, Inc., Burlington, MA, USA).

Ottawa Federal Fine sand was obtained from US Silica (Ottawa, IL, USA). Sandy aquifer materials were collected from Sandwich, MA as a composite sample of multiple cores in the interval of 8 to 10 feet below ground surface. Sandy aquifer materials were collected from Falmouth, MA at a depth of 4 to 12 feet below ground surface. Aquifer materials were stored in zip lock bags at -80 °C until used in the experiments.

The carbon source for the experiments was EVO SRS[®]-NR manufactured and provided by Terra Systems, Inc. (Claymont, DE, USA). Vegetable oil is a complex mixture of hydrocarbons, that when biodegraded produces a suite of more readily accessible organic compounds. For this reason, COD is used to track the substrate over time. While the use of COD precludes determination of the precise breakdown pathways of the complex carbon substrate, it is well aligned with the modeling approaches employed to examine denitrification [48].

2.2. Batch Experiments

Microcosm experiments are conducted in 1 L screw cap sealed glass reactors. Experiments 1 and 2 included control reactors conducted without oil and without soil and three treatment reactors. The contents of reactors used in Experiments 1 and 2 are shown in Table 1. Reactors containing soil from the Falmouth, MA site are labeled R01-R05, and reactors containing soil from the Sandwich, MA site are labeled RS1-RS5. Reactors were mixed at 22 ± 2 °C for between 10 and 25 days using shaker trays (New Brunswick Innova 2000 Platform Shaker, Eppendorf, Enfield, CT, USA).

Table 1. Microcosm contents for Experiments 1 and 2.

Reactor ID	Nitrate (mg-N/L)	Condition	EVO (mg/L)	Soil (g)	Water (mL)
R01	0.06	control	1216	50.9	502.1
R02	17.97	control	0	51.0	501.6
R03	17.79	treatment	1237	50.9	500.6
R04	18.41	treatment	1096	50.9	502.2
R05	17.55	treatment	1119	50.8	500.9
RS1	0.03	control	817	51.1	501.5
RS2	20.95	control	0	51.0	500.7
RS3	20.55	treatment	1099	50.7	501.2
RS4	21.24	treatment	1135	51.0	501.9
RS5	18.25	treatment	1038	50.8	500.4

Experiment 3 comprised of five tests, each using a series of reactors (Table 2) to explore the influence of pH 4, 7, 8 on biostimulation of denitrification. Tests at pH 4 were conducted using unadjusted and adjusted reactors. Tests conducted at pH 8 used adjusted reactors, while tests at pH 7 were unadjusted. Unadjusted reactors were initiated and allowed to

progress without an attempt to maintain pH. Adjusted reactors received either acid (1 M HCl) or base (0.1 M NaOH) daily to maintain pH at the target value.

Table 2. Microcosm compositions used in Experiment 3.

Target pH	Reactor ID	Nitrate (mg-N/L)	EVO (mg/L)	Water (mL)	Soil (g)	Soil Type
7.0 unadjusted	R10	6.8	3336	493.5	51.8	OS
	R11	5.3	3555	493.7	66.8	SS
7.0 unadjusted	R70	22.2	3336	493.5	51.8	OS
	R71	22.2	3555	493.7	66.8	SS
4.0 adjusted	R40	18.5	0	497.6	66.6	SS
	R41	15.0	422	497.4	66.9	SS
	R41D	15.6	221	497.6	69.2	SS
4.0 unadjusted	R20	19.5	0	497.6	66.4	SS
	R21	18.7	1084	498.0	66.9	SS
	R21D	18.8	1065	497.8	67.2	SS
8.0 adjusted	R80	17.1	0	248.5	32.2	SS
	R81	17.4	964	248.9	32	SS
	R81D	17.8	1247	248.7	32	SS

Note: Ottawa Sand (OS) and Sandwich Soil (SS).

2.3. Analytical Methods

pH was measured using a Thermo Scientific™ Orion™ Star A216 pH/DO meter with ROSS Ultra Triode epoxy-body pH/ATC electrode. Samples collected throughout the duration of the experiment were stored at $-80\text{ }^{\circ}\text{C}$ until the time of analysis. Nitrate and nitrite concentrations were quantified using a Dionex ICS 2000 Ion Chromatograph (Sunnyvale, CA, USA). Soluble COD samples were taken by filtering 3 mL of mixed sample through $0.45\text{ }\mu\text{m}$ filters and analyzed using a closed reflux, colorimetric method 8000 by HACH (Loveland, CO, USA), based on standard method 5220 D. UV absorbance at 620 nm was quantified using a Perkin Elmer Lambda 25 UV/vis spectrophotometer. Soil samples collected before and after the experiment were extracted for DNA using DNeasy PowerSoil® by Qiagen™. DNA was separated from other components of the soil sample by multiple steps following preservation instructions from the kit. Extracts were maintained at $-80\text{ }^{\circ}\text{C}$ until shipment to SiREM (Guelph, ON, Canada) for analysis. Total bacteria were quantified by the 16S rRNA gene count, present in all bacteria (copies per gram of wet soil). An assumption was made that each bacterial organism holds only one copy of this gene, although it is understood that some bacteria are documented to have more than one 16S rRNA gene copy [49].

2.4. ASM3 Modeling Approach

The ASM3 model [42] was used to evaluate microcosms using a two-step denitrification model. Components modeled include nitrate, nitrite, nitrogen (N_2), oxygen (O_2), complex carbon substrate, soluble substrate, and heterotrophic biomass. The ASM3 approach includes heterotrophic growth rates under aerobic and anoxic conditions. The EVO biodegradation was modeled in two steps. In step one, complex carbon (e.g., linoleic acid) is transformed into soluble substrate assumed to be acetate. In step two, soluble substrate is utilized by the organisms via the simplified storage product process described within the ASM framework [42]. The Kaelin et al. (2009) model contains 47 model parameters (Table 3) and 13 processes (Supplementary Material—Table S1). Values for the model parameters and model stoichiometry (Supplementary Material—Table S2) were obtained from the literature [42,43,48].

Table 3. Model parameters at 20 °C. Values from [42] unless otherwise noted.

Symbol	Characterization	Value	Units
$i_{N,SI}$	N content of inert soluble COD SI	0.01	[g N/g COD]
$i_{N,SS}$	N content of readily biodegradable substrate	0.03	[g N/g COD]
$i_{N,XI}$	N content of inert particulate COD X_I	0.04	[g N/g COD]
$i_{N,XS}$	N content of slowly biodegradable substrate	0.03	[g N/g COD]
$i_{N,BM}$	N content of biomass, X_H , X_A	0.07	[g N/g COD]
f_{SI}	Production of SI in hydrolysis	0.00	[g COD/g COD]
f_{XI}	Fraction of inert COD generated in biomass lysis	0.2	[g COD/g COD]
Y_{HO2}	Yield coeff. for heterotrophs in aerobic growth	0.8	[g COD/g COD]
Y_{HNO3}	Yield coeff., heterotrophic anoxic growth using NO_3	0.7	[g COD/g COD]
Y_{HNO2}	Yield coeff., heterotrophic anoxic growth using NO_2	0.7	[g COD/g COD]
Y_{STO2}	Yield coeff. for X_{STO} in aerobic growth	0.8	[g COD/g COD]
Y_{STONO3}	Yield coeff. for X_{STO} in anoxic growth using NO_3	0.7	[g COD/g COD]
Y_{STONO2}	Yield coeff. for X_{STO} in anoxic growth using NO_2	0.7	[g COD/g COD]
$\ _H$	Hydrolysis rate constant	9	[d^{-1}]
$\ _{sto}$	Maximum storage rate	12	[d^{-1}]
μ_H	Maximum growth rate on substrate	3	[d^{-1}]
b_{H,O_2}	Aerobic end. resp. rate for X_H	0.2	[d^{-1}] [43]
b_{STO,O_2}	Aerobic end. resp. rate for X_{STO}	0.3	[d^{-1}]
η_{H,NO_3}	Reduction factor for NO_3 reduction	0.2 (0.15–0.25)	-
η_{H,NO_2}	Reduction factor for NO_2 reduction	0.2 (0.15–0.25)	-
η_{H,end,NO_3}	Reduction factor for b_H using NO_3	0.4 (0.25–0.50)	-
η_{H,end,NO_2}	Reduction factor for b_H using NO_2	0.5 (0.35–0.70)	-
$\eta_{N,end}$	Reduction factor for b_{AOB} and b_{NOB} , anoxic	0.1	-
K_X	Hydrolysis half saturation constant	1.0	[$g X_S g^{-1} X_H$]
K_{H,O_2}	Saturation/inhibition coeff. for oxygen, het. growth	0.2	[$g O_2 m^{-3}$]
$K_{H,O_2,inh}$	Inhibition coefficient for oxygen, het. growth	0.2	[$g O_2 m^{-3}$]
$K_{H,SS}$	Saturation coeff. for readily biodegradableSubstrates	10	[$g COD m^{-3}$]
K_{H,NH_4}	Saturation/inhibition coefficient for ammonium	0.01	[$g N m^{-3}$]
K_{H,NO_3}	Saturation/inhibition coefficient for nitrate	0.5	[$g N m^{-3}$]
K_{H,NO_2}	Saturation/inhibition coefficient for nitrite	0.5	[$g N m^{-3}$]
$K_{H,NO_2,inh}$	Inhibition coefficient for nitrite	0.5	[$g N m^{-3}$]
$K_{H,ALK}$	Saturation coefficient for alkalinity	0.1	[$mole HCO_3^- m^{-3}$]
$K_{H,STO}$	Saturation coefficient for storage products	0.1	[$g COD m^{-3}$]

Initial conditions for the model simulations are shown in Table 4. Dissolved oxygen is present in all reactors at initial concentration of 6 mg/L and assumed to be rapidly consumed by bacteria given the presence of degradable carbon.

Table 4. Initial conditions used when modeling the reactors.

Component	Symbol	RS1	RS2	RS3	RS4	RS5
oxygen (mg/L)	S _{DO}	6	6	5	5	4
nitrate (mg-N/L)	S _{NO3}	0	20	20	20	20
nitrite (mg-N/L)	S _{NO2}	0	0	0	0	0
nitrogen (mg-N/L)	S _{N2}	0	0	0	0	0
ammonia (mg-N/L)	S _{NH}	0	0	0	0	0
EVO (mg-COD/L)	X _S	2860	0	2860	2860	2860
soluble substrate (mg-COD/L)	S _S	80	0	80	80	80
alkalinity (mole HCO ₃ /m ³)	Alk	0	0	0	0	0
particulate inert organic matter (mg-COD/L)	X _I	0	0	0	0	0
storage (mg-COD/L)	X _{STO}	0	0	0	0	0
heterotrophic biomass (mg-COD/L)	X _H			calibrated		

The model was written and executed in Matlab 2021a. Experimental data were fit by adjusting initial biomass concentration. Fits were obtained using the `lsqnonlin` function with an objective function of nitrate and nitrate sum squared differences.

3. Results and Discussions

3.1. Denitrification in Experiments Using Sandwich and Falmouth Material at Neutral pH

Data from Experiment 1, conducted using soil from Falmouth MA, show no appreciable changes in nitrate concentration over the 16-day duration of the experiment (Supplementary Materials—Figure S1). COD and pH were not limiting in this experiment. The limited denitrification observed in Experiment 1 is attributed to limited biomass associated with the sandy material, confirmed with lower biomass quantification in the aquifer material after the end of experiment.

Nitrate reduction was observed in Experiment 2, which was conducted using soil from Sandwich, MA (Figure 1). Despite the identical set up, reactors RS3, RS4 and RS5 showed different rates for nitrate reduction in the experiment, respectively 10.1, 2.62 and 6.01 mg/(L·d). Nitrate in Reactor RS5 was completely reduced in 2.7 days, while in reactors RS3 and RS4 nitrate was reduced by 39% and 64%, respectively, over the same period. The difference in behavior among the replicates is not fully understood, but we hypothesize that the physical and biological heterogeneity within the sample of Sandwich soil was a strong contributor to the observed behavior. The quantification of biomass in soil samples corroborate this hypothesis. In these experiments, soil was used without preparation (i.e., no washing, sieving, or mixing), and the Sandwich material was a composite sample from taken from seven different soil borings suggesting there may be a strong spatial gradient in the number of denitrifying bacteria present at the site. It should be noted here, that the PRB implementation may overcome lower spatially varying biomass concentrations through sustained periods of stimulation.

Nitrite accumulation was observed in Experiment 2 after day 1, though the concentrations (~2 mg/L for all but one sample) were not found to be limiting. Nitrite concentration began decreasing after day 5. Soluble COD decreased initially but increased at a near constant rate after day 5–6. The increasing concentrations of soluble substrate at the end of the experiment are indicative of sustained hydrolysis

Biomass and denitrifying genes, *nirK*, *nirS*, and *nosZ*, were quantified via qPCR in selected reactors from Experiment 2 (Figure 2). Nitrate reduction variation in the Sandwich experiment can be explained by the difference in denitrifier concentration among samples, specifically *nirS*. Initial (I) and final (F) samples from the same reactor were analyzed to quantify biomass growth during the experimental period. Nitrite reductases (*nirK* and *nirS*) are representative of the nitrite reduction, while nitrous oxide reductase (*nosZ*) is the target gene responsible for generating nitrogen gas.

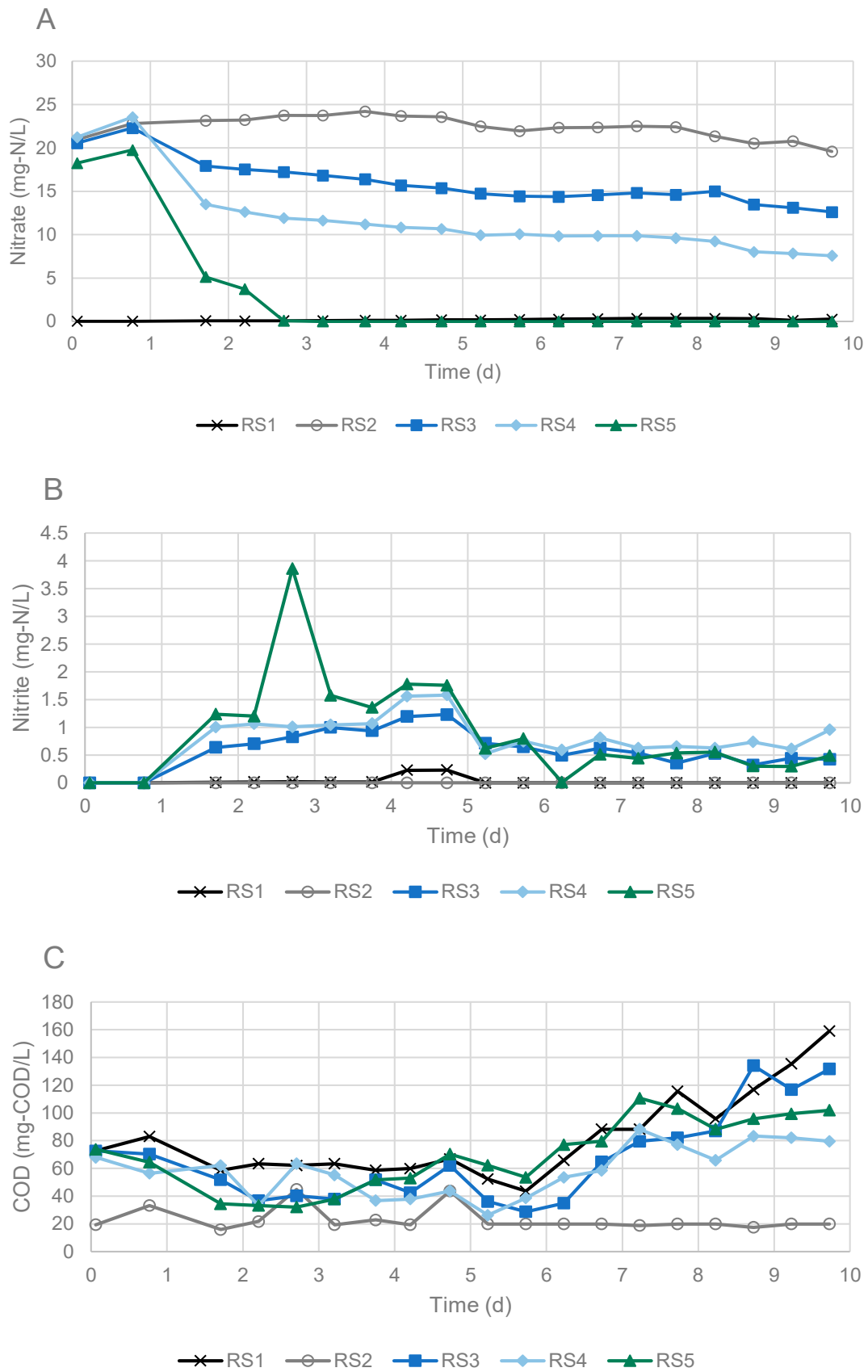


Figure 1. Data from Experiment 2: (A) nitrate; (B) nitrite (C) COD (RS1—control with no nitrate, RS2—control with no EVO, RS3, RS4, RS5—replicates of reactor with nitrate and EVO). Lines added to help visualize the trends in the data.

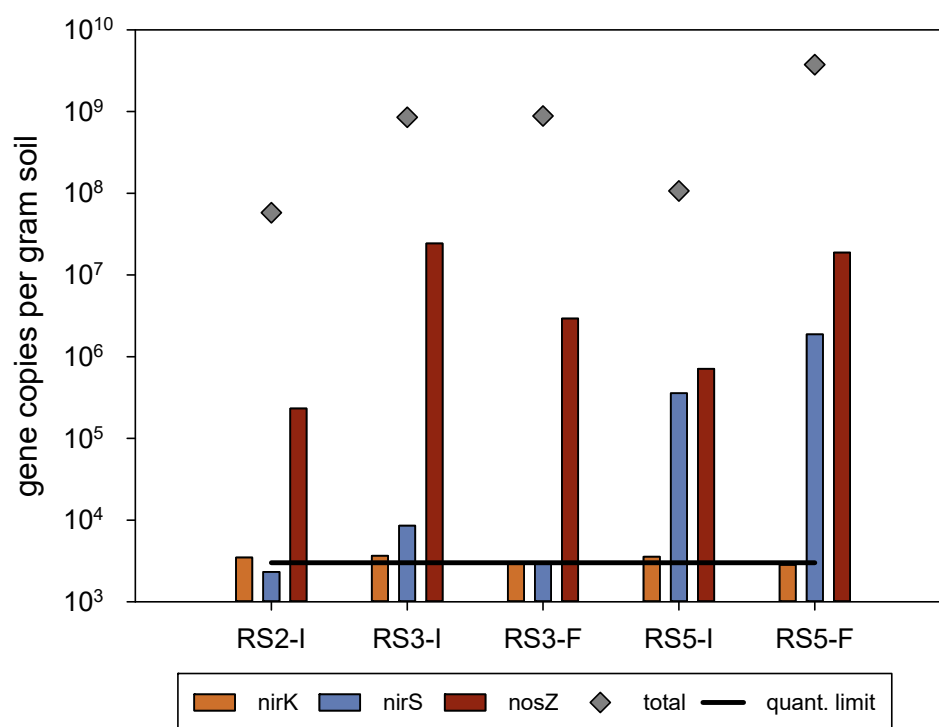
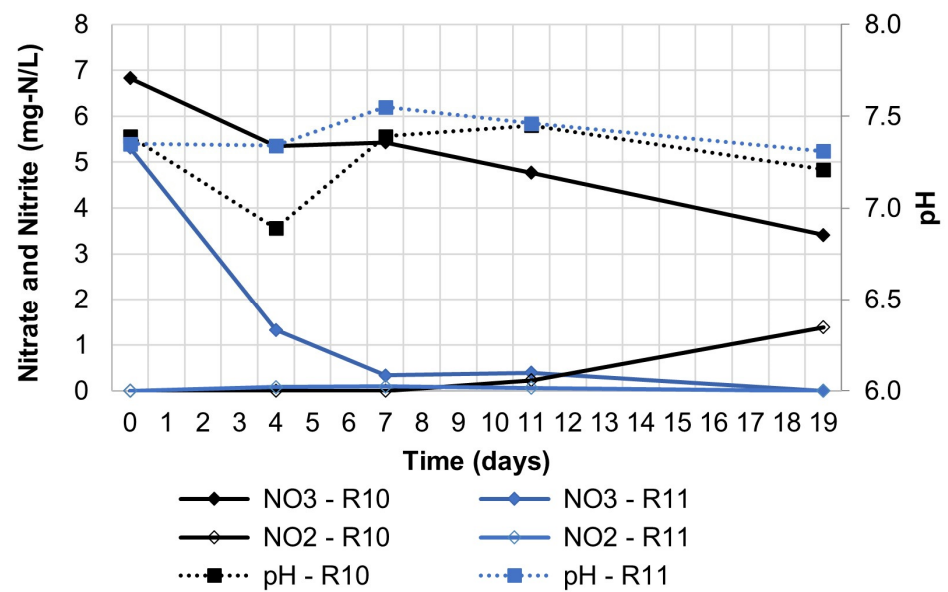


Figure 2. Biomass characterization results from Experiment 2.

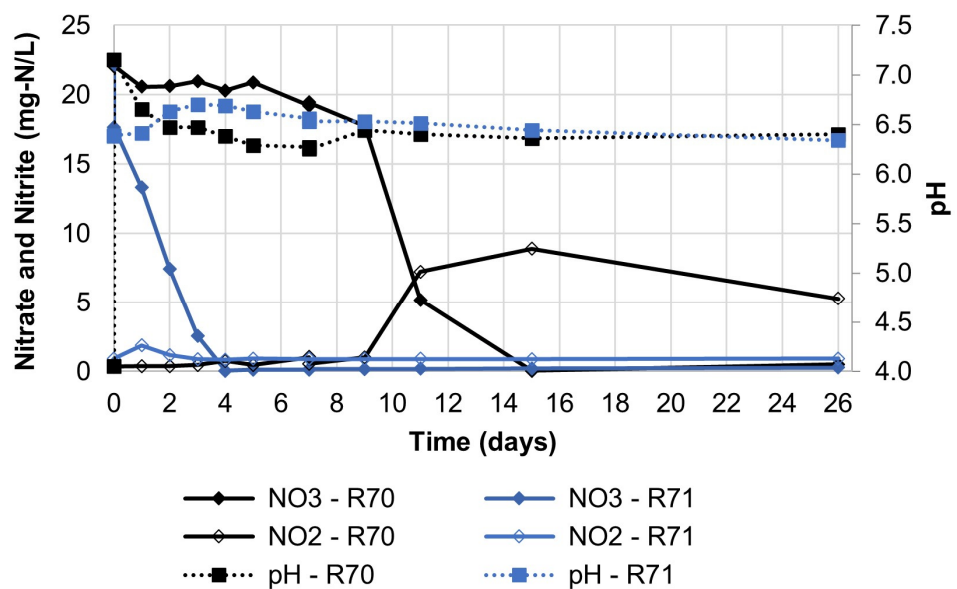
The total biomass in Experiment 2 using aquifer material collected from Sandwich was found to be one order of magnitude higher than biomass in Falmouth aquifer material. The nitrate reductase *nirS* was only detected in Sandwich soil samples, corroborating the hypothesis of a lower denitrification potential in Falmouth soil. The *nosZ* gene copies per gram were two orders of magnitude higher in the Sandwich experiment, indicating the difference in biological population between the two locations. The enzymes with *nirK* were not detected in any of the samples. The *nosZ* gene is known to have significantly higher frequency of co-occurrence with *nirS* than with *nirK* [50], which could explain the absence of *nirK* in these samples. Biomass quantification should be evaluated with caution since it is not necessarily correlated to bacterial activity. Based on a pure culture of *Paracoccus denitrificans*, a study by Baumann et al. [51] showed that decreased denitrification activity was not always followed by a decrease in target genes *narH*, *nirS*, and *nosZ* mRNA concentrations. Such tendency may not occur in naturally occurring bacteria in the medium used in experiments.

3.2. Influence of pH on Denitrification

Two tests were conducted with a neutral pH environment with material collected from Sandwich, MA, and Ottawa Sand. In these tests, the second set of reactors (R70/R71) was conducted one month after the first (R10/R11) by re-spiking the same reactors with nitrate. Total denitrification was observed in experiments with neutral pH. As shown in Figure 3, higher nitrate reduction rates were noted in microcosms containing Sandwich material (Reactors R71 and R11) than in those reactors containing Ottawa Sand (Reactors R70 and R10). In addition, rates of denitrification appear to be greater in the re-spiked reactors (R70/R71), which is thought to have resulted from a combination of greater biomass present and the availability of partially degraded EVO.



(A)



(B)

Figure 3. Data from reactors in Experiment 3 at pH 7: (A) initial test, (B) reintroduction of nitrate to reactors. Reactors R10/R70 contained Ottawa sand and reactors R11/R71 contained Sandwich aquifer material. Lines added to help visualize the trend in the data.

Results from tests at pH 8.0 suggest no appreciable effect of elevated pH when compared to the results obtained at pH 7.0. However, denitrification was not observed when pH was maintained near 4.0 in reactor set R40/R41/R41D (Figure 4C,D). In the unadjusted reactor set having initial pH 4.0 (R20/R21/R21D the pH was observed to increase over time (Figure 4A,B), with nitrate reduction occurring rapidly once pH exceeded a value of 5. The increase in pH is consistent with the utilization of acetate as an electron donor [25,52].

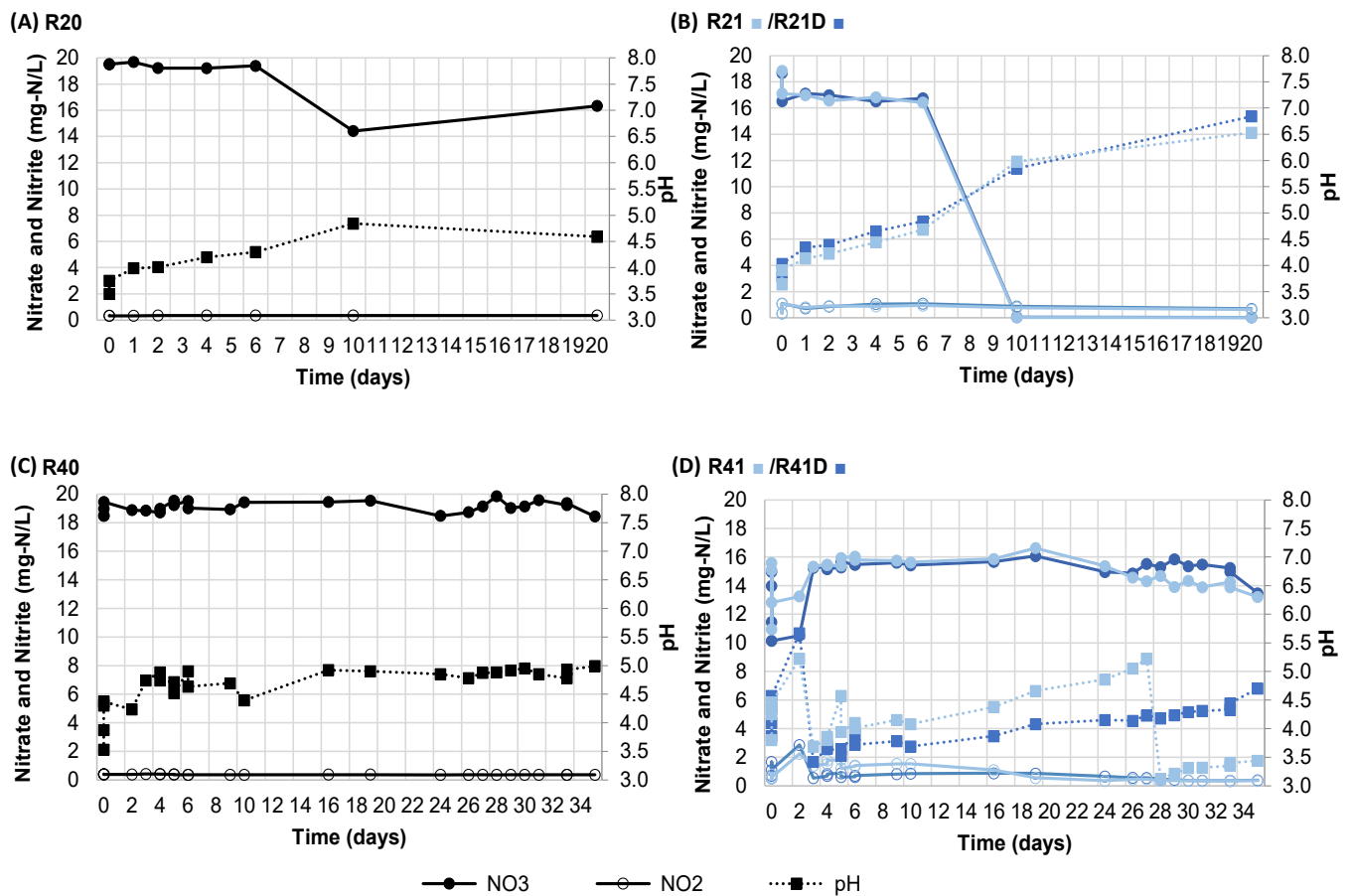


Figure 4. Data from Sandwich soil reactors in Experiment 3 at pH 4: (A) control without EVO, no pH adjustment; (B) treatment replicates, no pH adjustment; (C) control without EVO, pH maintained at 4 via acid addition; and (D) treatment replicates, pH maintained at 4 via acid addition. Lines added to help visualize the trend in the data.

3.3. Model Results

Results from Experiment 2 were used to calibrate the model by adjusting initial biomass, nitrite inhibition, and hydrolysis parameters. The initial biomass was adjusted based on the uncertainty in the quantification of biomass via qPCR [53]. Nitrite inhibition was adjusted because initial simulations indicated the biomass populations stimulated from the subsurface materials were more sensitive to nitrite than is otherwise seen when modeling denitrification in water resource recovery facilities. The hydrolysis parameters were adjusted on the basis that the emulsified vegetable oil is more complex than C1–C3 carbons typically used to support denitrification in water resource recovery facilities. Fitted parameter values are shown in Table 5. The hydrolysis rate k_{X5} and the half saturation of soluble substrate K_S were selected for calibration for being substrate specific parameters relevant to describe the slow release of carbon from EVO.

Results for the calibration of the model to the three treatment reactors in Experiment 2 are shown in Table 5 and Figures 5–7. Initial biomass was fit separately in each reactor, given that denitrification rates were different among replicates. Single values of all other fitting parameters were obtained.

Table 5. Parameters fit to Experiment 2.

Parameter	Symbol	Fitted Value	Initial Guess	Literature Value
initial biomass (mg-COD/L)				
RS3	X_H	1.10	2	not applicable
RS4		2.56	2	
RS5		18.9	20	
nitrite inhibition (mg-N/L)	K_{iNO_2}	0.0123	0.1	0.2 ¹ [42]
half saturation for Ss (mg-COD/L)	$K_{H,SS}$	66.91	65	10 [43] 10–180 [54] 2 [48]
hydrolysis rate constant (d ⁻¹)	k_{XS}	0.86	1	3 [43] 9 [42]

Note: ¹ Created coefficient based on oxygen inhibition.

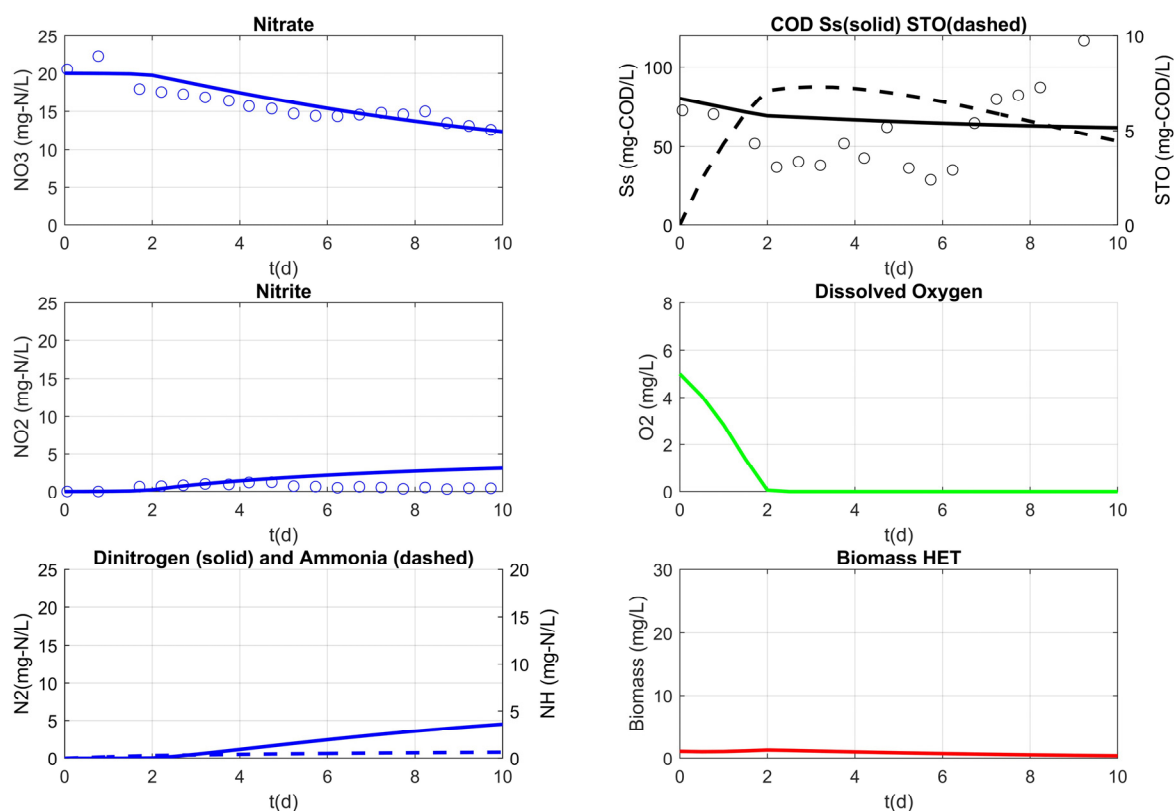


Figure 5. Model output for reactor RS3, describing variations over time for nitrate, nitrite, dinitrogen and ammonia, COD and STO, dissolved oxygen, and heterotrophic biomass. Experiment measurements are shown as circles and the model is shown in solid or dashed lines.

Overall, the model well describes the data from the three experiments; however, the description of RS5 is superior to those provided for RS3 and RS4. This may have to do with the greater amount of denitrification observed in RS5. While nitrate data from all three experiments appeared to have a lag, denitrification occurred more quickly in RS5 and thus the lag has less influence on model performance. While there were appreciable differences in biomass in these reactors (as noted previously), these experiments were initiated in an environment containing some dissolved oxygen. The presence of dissolved oxygen at the start of the experiment may have also contributed to the observed lag. Once the oxygen was

consumed, the corresponding inhibition parameter no longer controlled the process rate and nitrate reduction commenced within the model calculations. The oxygen inhibition parameter used (0.2 mg O₂-/L [42]) is consistent with a microcosm environment considered perfectly mixed. In groundwater, however, it is known that denitrification can occur in oxygen concentrations of 1 or 2 mg/L [55] mostly due to the presence of micro-anaerobic environments formed by the distribution of particulate organic matter, heterogeneous organic-rich patches of sediments or biofilms. These denitrification hotspots may account for up to 90% of the denitrification activity representing only 1% of the soil volume [56]. Thus, future study should aim to understand the influence of spatially nonuniform mass flows of oxygen into the reactive zone within a PRB.

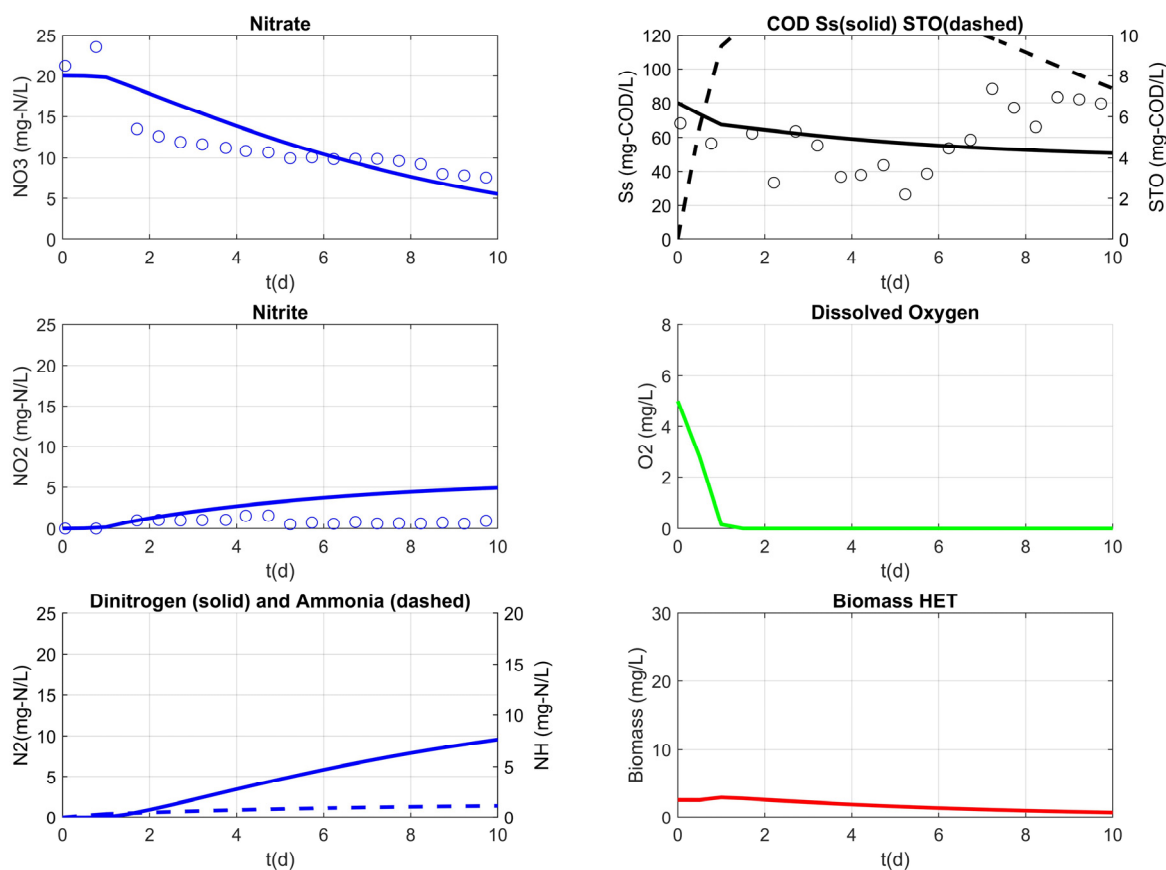


Figure 6. Model output for reactor RS4, describing variations over time for nitrate, nitrite, dinitrogen and ammonia, COD and STO, dissolved oxygen, and heterotrophic biomass. Experiment measurements are shown as circles and the model is shown in solid or dashed lines.

Soluble COD and storage (STO) show how the model describes heterotrophic utilization of organic carbon. Comparison of the model results for soluble COD with those measured the experiments suggests the model describes carbon processing. While trends in RS3 and RS4 are less apparent, soluble COD in RS5 increased at a later time, suggesting that soluble COD was produced but not consumed after nitrate was consumed.

The goal in fitting the batch experiments shown in Figures 5–7 was the development of a set of biokinetic parameters for subsequent use in simulating denitrification in PRBs. This was accomplished in the fitted values shown in Table 5 Attention was subsequently placed on simulating the unadjusted reactor having initial pH 4 from Experiment 3 using the biokinetic parameters produced from fitting the model to Experiment 2. The goal in simulating Experiment 3 is to describe the influence of pH on the denitrification process. Modeling pH within a microcosm can be complex, requiring a solution of acid-base equilibria in conjunction with soil buffering capacity and microbial processes. While a mechanistic

approach including these aspects may be meaningful for the ultimate application to PRB design and operation, it was beyond the scope of this research. In the absence of the mechanistic pH model, the pH data were input to the model as continuous linear function. This empirical approach informs the model of reactor pH with minimal computational overhead. Based on data observations, pH increase was linear during the 20 days of experiment, so the model describes pH variation as zero-order in time.

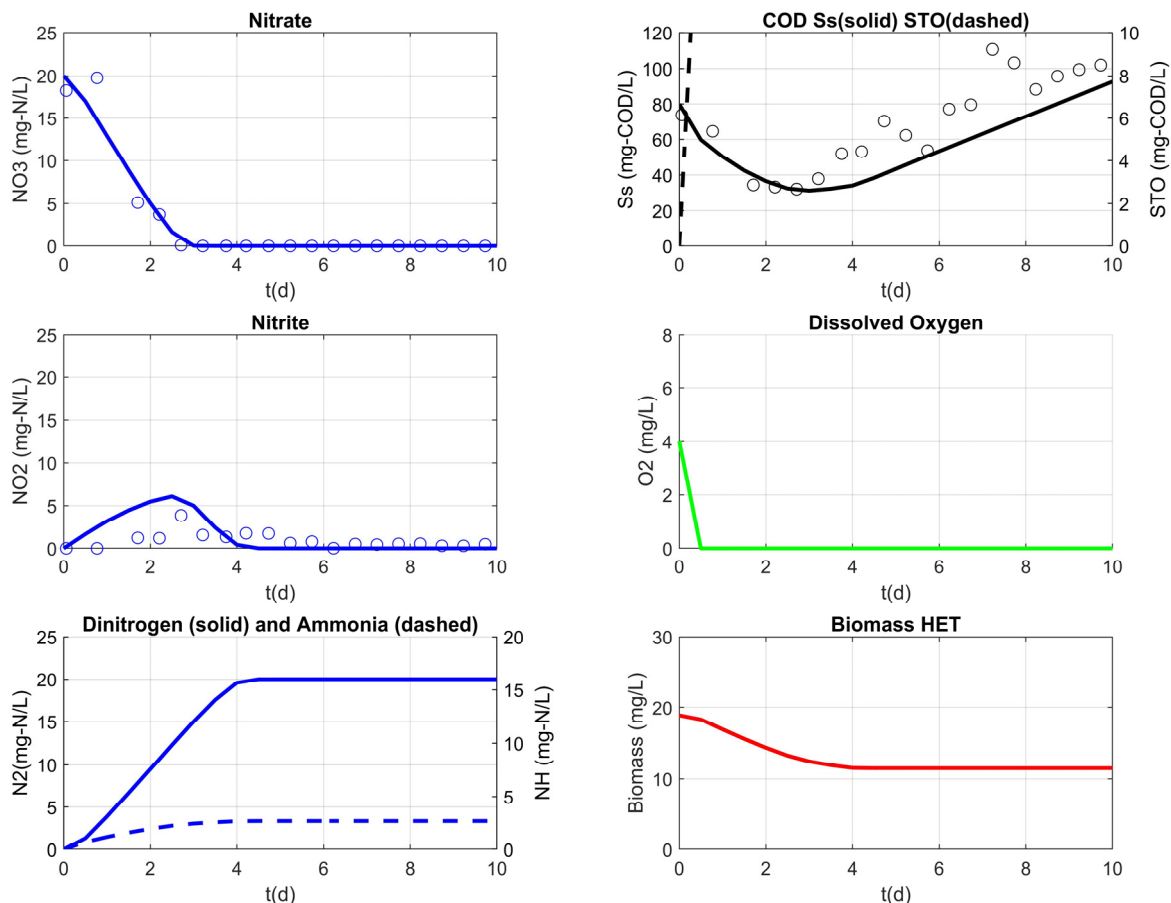


Figure 7. Model output for reactor RS5, describing variations over time for nitrate, nitrite, dinitrogen and ammonia, COD and STO, dissolved oxygen, and heterotrophic biomass. Experiment measurements are shown as circles and the model is shown in solid or dashed lines.

More important to capture within the model is the influence of pH on the denitrification process. Most nitrate reduction occurred between pH 4.5 and 5.5, suggesting there is a threshold in pH where pH limitation becomes less relevant, and denitrification rates are similar to neutral pH experiments. To capture this the process-based model was modified to include the sigmoidal pH limitation term (I_{pH}) shown in Equation (2).

$$I_{pH} = \frac{1}{1 + e^{-a \times b + b \times pH}} \tag{2}$$

where a is the inflection point in pH effect and b is a measure of steepness of the sigmoid curve. The pH limitation term returns a value between 0 and 1 depending on the pH in the reactor and modifies all process rates shown in Table 4. Parameters a and b were fit (4.98 and -8.63 , respectively) using the data from the unadjusted pH 4 reactor with no other adjustable parameters. That is, all previously-determined model parameters remained fixed. Fitted values of were used for a and b , respectively.

Model results indicate that at pH below 5.0 bacterial growth and nitrate reduction were limited. Above pH 5, nitrite was readily reduced. Nitrite accumulation reached a maximum

of 6 mg-N/L around day 9 before being readily degraded following the elimination of nitrate.

4. Implications

Our research focuses on quantifying denitrification biokinetics in microcosms established with aquifer materials collected from Cape Cod, MA and stimulated using emulsified vegetable oil. Results suggest that a variation in the observed rates of denitrification may be attributed to the variability of denitrifiers within the aquifer material. Thus, characterization efforts at sites being considered for PRB establishment using EVO should include the assessment of denitrifier populations prior to EVO injection. By evaluating three target genes of denitrification (*nirS*, *nirK*, *nosZ*), the presence of nitrite reductase (*nirS*) was found to be the best indicator of denitrification potential. As the cost for qPCR analysis can be an obstacle at the field scale, our results suggest selecting only one target gene (*nirS*) may be an option for evaluating denitrification potential at sites where PRBs are being considered.

With effective biostimulation and plentiful carbon, there appears limited reason to be concerned about nitrite posing a risk. Nitrite concentrations of approximately 2 mg/L in batch systems were observed. That notwithstanding, nitrite is known to inhibit many microbiological process [35] and any discharge of nitrite down gradient from a denitrifying PRB may drive concern regarding secondary effects of treatment. Thus, nitrite mass discharge from installations of denitrifying PRBs should be monitored to ensure the PRB performance results in complete denitrification.

Where pH increases above 8.0 due to denitrification, buffering agents may be needed [25]. However, biodegradation of the EVO will yield fatty acids that tend to reduce the pH. Our data show that in neutral pH reactors, nitrate reduction is not causing pH to appreciably increase and there appears to be little difference in kinetics between experiments conducted at pH 7 and pH 8. The limited increase in pH in circa neutral experiments suggest that buffering agents may not be needed when using emulsified oil in field settings where the groundwater pH is neutral to slightly acidic (>pH 5.0). Based on our results indicating limited denitrification below pH 5, lab-scale treatability tests are recommended when groundwater pH is below 5. What remains unanswered in this regard is whether pH gradients may set up within denitrifying PRBs established using EVO in acidic groundwater such that pH adjustments become unnecessary during longer-term treatment. Our results suggest this possibility should be explored in follow on research, and the development and application of the pH limitation term within this work may aid these studies.

The process-based model employed herein has potential to aid in PRB design and monitoring. This is important because additional research is needed to understand the broader suite of possible secondary effects. Greater incorporation of target genes along the denitrification pathway coupled with more sophisticated denitrification models [57] can aid the evaluation of PRBs in relation to greenhouse gases. Secondary effects are not limited to greenhouse gas considerations, but also include broader water quality concerns related to nitrite accumulation and COD discharge both of which are accessible via the modeling approach employed in this work.

Supplementary Materials: The following supporting information can be downloaded at: <https://www.mdpi.com/article/10.3390/w15050883/s1>, Figure S1. Experiment 1: (A) nitrate; (B) nitrite (C) COD (R01—control with no nitrate, R02—control with no EVO, R03, R04, R05—replicates of reactor with nitrate and EVO). Table S1. Process rate equations used in the model. Table S2. Model stoichiometry [38].

Author Contributions: V.L.G.: investigation, methodology, software, writing—original draft; P.M.D.: conceptualization, resources, writing—review and editing; M.D.L.: conceptualization, writing—review and editing; C.A.R.: conceptualization, resources, supervision; writing—review and editing. All authors have read and agreed to the published version of the manuscript.

Funding: Funding for this work was provided through discretionary resources managed by C.A.R. at Tufts University.

Institutional Review Board Statement: Not applicable.

Informed Consent Statement: Not applicable.

Data Availability Statement: The data presented in this study are available from the corresponding author upon request.

Acknowledgments: We gratefully acknowledge the helpful suggestions provided by the reviewers. In kind contributions of materials and supplies were provided by ISOTEC and Terra Systems, Inc. The authors express appreciation to Horsley Witten Group for collection of the aquifer materials used in this work.

Conflicts of Interest: C. Andrew Ramsburg and Veronica Lima Gonzalez declare no conflict of interest. Paul M. Dombrowski is Director and Senior Remediation Engineer at ISOTEC. Michael D. Lee is Vice President of Research and Development at Terra Systems.

References

1. Robertson, W.D.; Blowes, D.W.; Ptacek, C.J.; Cherry, J.A. Long-Term Performance of In Situ Reactive Barriers for Nitrate Remediation. *Ground Water* **2000**, *38*, 689–695. [[CrossRef](#)]
2. Korom, S.F. Natural Denitrification in the Saturated Zone: A Review. *Water Resour. Res.* **1992**, *28*, 1657–1668. [[CrossRef](#)]
3. Lu, H.; Chandran, K. Diagnosis and Quantification of Glycerol Assimilating Denitrifying Bacteria in an Integrated Fixed-Film Activated Sludge Reactor via ¹³C DNA Stable-Isotope Probing. *Environ. Sci. Technol.* **2010**, *44*, 8943–8949. [[CrossRef](#)] [[PubMed](#)]
4. Dahab, M.F. Comparison and Evaluation of In-Situ Bio-Denitrification Systems for Nitrate Reduction in Groundwater. *Water Sci. Technol.* **1993**, *28*, 359–368. [[CrossRef](#)]
5. Hunter, W.J. Use of Vegetable Oil in a Pilot-Scale Denitrifying Barrier. *J. Contam. Hydrol.* **2001**, *53*, 119–131. [[CrossRef](#)]
6. Friedman, L.; Mamane, H.; Avisar, D.; Chandran, K. The Role of Influent Organic Carbon-to-Nitrogen (COD/N) Ratio in Removal Rates and Shaping Microbial Ecology in Soil Aquifer Treatment (SAT). *Water Res.* **2018**, *146*, 197–205. [[CrossRef](#)]
7. Slater, J.M.; Capone, D.G. Denitrification in Aquifer Soil and Nearshore Marine Sediments Influenced by Groundwater Nitrate. *Appl. Environ. Microbiol.* **1987**, *53*, 1292–1297. [[CrossRef](#)]
8. Slater, L.; Binley, A. Evaluation of Permeable Reactive Barrier (PRB) Integrity Using Electrical Imaging Methods. *Geophysics* **2003**, *68*, 911–921. [[CrossRef](#)]
9. Faisal, A.A.H.; Sulaymon, A.H.; Khaliefa, Q.M. A Review of Permeable Reactive Barrier as Passive Sustainable Technology for Groundwater Remediation. *Int. J. Environ. Sci. Technol.* **2018**, *15*, 1123–1138. [[CrossRef](#)]
10. Robertson, W.D.; Cherry, J.A. In Situ Denitrification of Septic-System Nitrate Using Reactive Porous Media Barriers: Field Trials. *Ground Water* **1995**, *33*, 99–111. [[CrossRef](#)]
11. Hiortdahl, K.M.; Borden, R.C. Enhanced Reductive Dechlorination of Tetrachloroethene Dense Nonaqueous Phase Liquid with EVO and Mg(OH)₂. *Environ. Sci. Technol.* **2014**, *48*, 624–631. [[CrossRef](#)] [[PubMed](#)]
12. Harkness, M.; Fisher, A. Use of Emulsified Vegetable Oil to Support Bioremediation of TCE DNAPL in Soil Columns. *J. Contam. Hydrol.* **2013**, *151*, 16–33. [[CrossRef](#)] [[PubMed](#)]
13. Tang, G.; Wu, W.-M.; Watson, D.B.; Parker, J.C.; Schadt, C.W.; Shi, X.; Brooks, S.C. U(VI) Bioreduction with Emulsified Vegetable Oil as the Electron Donor—Microcosm Tests and Model Development. *Environ. Sci. Technol.* **2013**, *47*, 3209–3217. [[CrossRef](#)] [[PubMed](#)]
14. Sleep, B.E.; Seepersad, D.J.; Mo, K.; Heidorn, C.M.; Hrapovic, L.; Morrill, P.L.; McMaster, M.L.; Hood, E.D.; LeBron, C.; Sherwood Lollar, B.; et al. Biological Enhancement of Tetrachloroethene Dissolution and Associated Microbial Community Changes. *Environ. Sci. Technol.* **2006**, *40*, 3623–3633. [[CrossRef](#)]
15. Lee, M.D.; Hostrop, F.; Hauptmann, E.; Raymond, R., Jr.; Begley, J.F. Column Studies to Evaluate EVO for Nitrate Removal in Permeable Reactive Barriers on Cape Cod, MA. In Proceedings of the Remediation of Chlorinated and Recalcitrant Compounds—2016, Palm Springs, CA, USA, 22–26 May 2016; Battelle Memorial Institute: Columbus, OH, USA, 2016.
16. Berge, N.D.; Ramsburg, C.A. Oil-in-Water Emulsions for Encapsulated Delivery of Reactive Iron Particles. *Environ. Sci. Technol.* **2009**, *43*, 5060–5066. [[CrossRef](#)]
17. Muller, K.A.; Esfahani, S.G.; Chapra, S.C.; Ramsburg, C.A. Transport and Retention of Concentrated Oil-in-Water Emulsions in Porous Media. *Environ. Sci. Technol.* **2018**, *52*, 4256–4264. [[CrossRef](#)]
18. Coulibaly, K.M.; Long, C.M.; Borden, R.C. Transport of Edible Oil Emulsions in Clayey Sands: One-Dimensional Column Results and Model Development. *J. Hydrol. Eng.* **2006**, *11*, 230–237. [[CrossRef](#)]
19. Crocker, J.J.; Berge, N.D.; Ramsburg, C.A. Encapsulated Delivery of Reactive Iron Particles Using Oil-in-Water Emulsions. In Proceedings of the Securing Groundwater Quality in Urban and Industrial Environments; IAHS Press: Fremantle, Australia, 2008; pp. 242–249.
20. Coulibaly, K.M.; Borden, R.C. Impact of Edible Oil Injection on the Permeability of Aquifer Sands. *J. Contam. Hydrol.* **2004**, *71*, 219–237. [[CrossRef](#)]

21. Dong, J.; Yu, D.; Li, Y.; Li, B.; Bao, Q. Transport and Release of Electron Donors and Alkalinity during Reductive Dechlorination by Combined Emulsified Vegetable Oil and Colloidal $Mg(OH)_2$: Laboratory Sand Column and Microcosm Tests. *J. Contam. Hydrol.* **2019**, *225*, 103501. [[CrossRef](#)]
22. Smith, R.L.; Duff, J.H. Denitrification in a Sand and Gravel Aquifer. *Appl. Environ. Microbiol.* **1988**, *54*, 8. [[CrossRef](#)]
23. Cape Cod Commission Section 208 Plan-Cape Cod Area Wide Water Quality Management Plan Update 2015. Available online: https://www.capecodcommission.org/resource-library/file/?url=/dept/commission/team/208/208%20Final/Cape_Cod_Area_Wide_Water_Quality_Management_Plan_Update_June_15_2015.pdf (accessed on 23 February 2023).
24. Rakhimbekova, S.; O'Carroll, D.M.; Oldfield, L.E.; Ptacek, C.J.; Robinson, C.E. Spatiotemporal Controls on Septic System Derived Nutrients in a Nearshore Aquifer and Their Discharge to a Large Lake. *Sci. Total Environ.* **2021**, *752*, 141262. [[CrossRef](#)] [[PubMed](#)]
25. Rust, C. Control of PH during Denitrification in Subsurface Sediment Microcosms Using Encapsulated Phosphate Buffer. *Water Res.* **2000**, *34*, 1447–1454. [[CrossRef](#)]
26. Borden, R.C. Effective Distribution of Emulsified Edible Oil for Enhanced Anaerobic Bioremediation. *J. Contam. Hydrol.* **2007**, *94*, 1–12. [[CrossRef](#)]
27. Borden, R.C.; Rodriguez, B.X. Evaluation of Slow Release Substrates for Anaerobic Bioremediation. *Bioremediation J.* **2006**, *10*, 59–69. [[CrossRef](#)]
28. Duhamel, M.; Wehr, S.D.; Yu, L.; Rizvi, H.; Seepersad, D.; Dworatzek, S.; Cox, E.E.; Edwards, E.A. Comparison of Anaerobic Dechlorinating Enrichment Cultures Maintained on Tetrachloroethene, Trichloroethene, Cis-Dichloroethene and Vinyl Chloride. *Water Res.* **2002**, *36*, 4193–4202. [[CrossRef](#)]
29. Löffler, F.E.; Cole, J.R.; Ritalahti, K.M.; Tiedje, J.M. Diversity of Dechlorinating Bacteria. In *Dehalogenation: Microbial Processes and Environmental Applications*; Häggblom, M.M., Bossert, I.D., Eds.; Springer: Boston, MA, USA, 2003; pp. 53–87. ISBN 978-0-306-48011-9.
30. Gihring, T.M.; Zhang, G.; Brandt, C.C.; Brooks, S.C.; Campbell, J.H.; Carroll, S.; Criddle, C.S.; Green, S.J.; Jardine, P.; Kostka, J.E.; et al. A Limited Microbial Consortium Is Responsible for Extended Bioreduction of Uranium in a Contaminated Aquifer. *Appl. Environ. Microbiol.* **2011**, *77*, 5955–5965. [[CrossRef](#)]
31. Calderer, M.; Jubany, I.; Pérez, R.; Martí, V.; de Pablo, J. Modelling Enhanced Groundwater Denitrification in Batch Microcosm Tests. *Chem. Eng. J.* **2010**, *165*, 2–9. [[CrossRef](#)]
32. Kornaros, M.; Lyberatos, G. Kinetic Modelling of Pseudomonas Denitrificans Growth and Denitrification under Aerobic, Anoxic and Transient Operating Conditions. *Water Res.* **1998**, *32*, 1912–1922. [[CrossRef](#)]
33. Mekala, C.; Nambi, I.M. Transport of Ammonium and Nitrate in Saturated Porous Media Incorporating Physiobiotransformations and Bioclogging. *Bioremediation J.* **2016**, *20*, 117–132. [[CrossRef](#)]
34. Clement, T.P.; Peyton, B.M.; Skeen, R.S.; Jennings, D.A.; Petersen, J.N. Microbial Growth and Transport in Porous Media under Denitrification Conditions: Experiments and Simulations. *J. Contam. Hydrol.* **1997**, *24*, 269–285. [[CrossRef](#)]
35. Glass, C.; Silverstein, J. Denitrification Kinetics of High Nitrate Concentration Water: PH Effect on Inhibition and Nitrite Accumulation. *Water Res.* **1998**, *32*, 831–839. [[CrossRef](#)]
36. Lu, B.; Liu, X.; Dong, P.; Tick, G.R.; Zheng, C.; Zhang, Y.; Mahmood-UI-Hassan, M.; Bai, H.; Lamy, E. Quantifying Fate and Transport of Nitrate in Saturated Soil Systems Using Fractional Derivative Model. *Appl. Math. Model.* **2020**, *81*, 279–295. [[CrossRef](#)]
37. Rodríguez-Escales, P.; Folch, A.; van Breukelen, B.M.; Vidal-Gavilan, G.; Sanchez-Vila, X. Modeling Long Term Enhanced in Situ Bionitrification and Induced Heterogeneity in Column Experiments under Different Feeding Strategies. *J. Hydrol.* **2016**, *538*, 127–137. [[CrossRef](#)]
38. Sun, Y.; Petersen, J.N.; Clement, T.P.; Hooker, B.S. Effect of Reaction Kinetics on Predicted Concentration Profiles during Subsurface Bioremediation. *J. Contam. Hydrol.* **1998**, *31*, 359–372. [[CrossRef](#)]
39. Wang, J.; Ma, R.; Guo, Z.; Qu, L.; Yin, M.; Zheng, C. Experiment and Multicomponent Model Based Analysis on the Effect of Flow Rate and Nitrate Concentration on Denitrification in Low-Permeability Media. *J. Contam. Hydrol.* **2020**, *235*, 103727. [[CrossRef](#)] [[PubMed](#)]
40. Killingstad, M.W.; Widdowson, M.A.; Smith, R.L. Modeling Enhanced In Situ Denitrification in Groundwater. *J. Environ. Eng.* **2002**, *128*, 491–504. [[CrossRef](#)]
41. Smith, R.L.; Miller, D.N.; Brooks, M.H.; Widdowson, M.A.; Killingstad, M.W. In Situ Stimulation of Groundwater Denitrification with Formate to Remediate Nitrate Contamination. *Environ. Sci. Technol.* **2001**, *35*, 196–203. [[CrossRef](#)]
42. Kaelin, D.; Manser, R.; Rieger, L.; Eugster, J.; Rottermann, K.; Siegrist, H. Extension of ASM3 for Two-Step Nitrification and Denitrification and Its Calibration and Validation with Batch Tests and Pilot Scale Data. *Water Res.* **2009**, *43*, 1680–1692. [[CrossRef](#)]
43. Koch, G.; Kühni, M.; Gujer, W.; Siegrist, H. Calibration and Validation of Activated Sludge Model No. 3 for Swiss Municipal Wastewater. *Water Res.* **2000**, *34*, 3580–3590. [[CrossRef](#)]
44. Ni, B.-J.; Rusalleda, M.; Pellicer-Nacher, C.; Smets, B.F. Modeling Nitrous Oxide Production during Biological Nitrogen Removal via Nitrification and Denitrification: Extensions to the General ASM Models. *Environ. Sci. Technol.* **2011**, *45*, 7768–7776. [[CrossRef](#)]
45. Ni, B.-J.; Yu, H.-Q. An Approach for Modeling Two-Step Denitrification in Activated Sludge Systems. *Chem. Eng. Sci.* **2008**, *63*, 1449–1459. [[CrossRef](#)]
46. Lu, H.; Chandran, K.; Stensel, D. Microbial Ecology of Denitrification in Biological Wastewater Treatment. *Water Res.* **2014**, *64*, 237–254. [[CrossRef](#)] [[PubMed](#)]

47. Perez-Garcia, O.; Mankelov, C.; Chandran, K.; Villas-Boas, S.G.; Singhal, N. Modulation of Nitrous Oxide (N₂O) Accumulation by Primary Metabolites in Denitrifying Cultures Adapting to Changes in Environmental C and N. *Environ. Sci. Technol.* **2017**, *51*, 13678–13688. [[CrossRef](#)] [[PubMed](#)]
48. Gujer, W.; Henze, M.; Mino, T.; van Loosdrecht, M. Activated Sludge Model No. 3. *Water Sci. Technol.* **1999**, *39*, 189–193. [[CrossRef](#)]
49. Jenkins, C.; Ling, C.L.; Ciesielczuk, H.L.; Lockwood, J.; Hopkins, S.; McHugh, T.D.; Gillespie, S.H.; Kibbler, C.C. Detection and Identification of Bacteria in Clinical Samples by 16S rRNA Gene Sequencing: Comparison of Two Different Approaches in Clinical Practice. *J. Med. Microbiol.* **2012**, *61*, 483–488. [[CrossRef](#)] [[PubMed](#)]
50. Graf, D.R.H.; Jones, C.M.; Hallin, S. Intergenomic Comparisons Highlight Modularity of the Denitrification Pathway and Underpin the Importance of Community Structure for N₂O Emissions. *PLoS ONE* **2014**, *9*, e114118. [[CrossRef](#)]
51. Baumann, B.; van der Meer, J.R.; Snozzi, M.; Zehnder, A.J.B. Inhibition of Denitrification Activity but Not of mRNA Induction in *Paracoccus denitrificans* by Nitrite at a Suboptimal pH. *Antonie Van Leeuwenhoek* **1997**, *72*, 183–189. [[CrossRef](#)]
52. Drtil, M.; Németh, P.; Kucman, K.; Bodík, I.; Kašperek, V. Acidobasic Balances in the Course of Heterotrophic Denitrification. *Water Res.* **1995**, *29*, 1353–1360. [[CrossRef](#)]
53. Henry, S.; Baudoin, E.; López-Gutiérrez, J.C.; Martin-Laurent, F.; Brauman, A.; Philippot, L. Quantification of Denitrifying Bacteria in Soils by NirK Gene Targeted Real-Time PCR. *J. Microbiol. Methods* **2004**, *59*, 327–335. [[CrossRef](#)]
54. Henze, M.; Grady, C.P.L.; Gujer, W.; Marais, G.V.R.; Matsuo, T. A General Model for Single-Sludge Wastewater Treatment Systems. *Water Res.* **1987**, *21*, 505–515. [[CrossRef](#)]
55. Rivett, M.O.; Buss, S.R.; Morgan, P.; Smith, J.W.N.; Benment, C.D. Nitrate Attenuation in Groundwater: A Review of Biogeochemical Controlling Processes. *Water Res.* **2008**, *42*, 4215–4232. [[CrossRef](#)] [[PubMed](#)]
56. Parkin, T.B. Soil Microsites as a Source of Denitrification Variability 1. *Soil Sci. Soc. Am. J.* **1987**, *51*, 1194–1199. [[CrossRef](#)]
57. Pan, Y.; Ni, B.-J.; Lu, H.; Chandran, K.; Richardson, D.; Yuan, Z. Evaluating Two Concepts for the Modelling of Intermediates Accumulation during Biological Denitrification in Wastewater Treatment. *Water Res.* **2015**, *71*, 21–31. [[CrossRef](#)] [[PubMed](#)]

Disclaimer/Publisher's Note: The statements, opinions and data contained in all publications are solely those of the individual author(s) and contributor(s) and not of MDPI and/or the editor(s). MDPI and/or the editor(s) disclaim responsibility for any injury to people or property resulting from any ideas, methods, instructions or products referred to in the content.